

Acknowledgments

We thank Ms. T. Kubo for technical assistance with the immunohistochemical staining, and Mr. K. Matsuda, KEYENCE, for the fluorescence microscope imaging, and analysis. This work was supported in part by a Grant-in-Aid for Scientific Research (C) from the Japanese Ministry of Education and Science (Grant No. 22590363 to T.I.).

References

1. Carroll, M.C. The complement system in regulation of adaptive immunity. *Nat Immunol* 2004;5:981–986.
2. Markiewski MM, DeAngelis RA, Benencia F, Ricklin-Lichtsteiner SK, Koutoulaki A, G. Coukos, et al. Modulation of the antitumor immune response by complement. *Nature Immunol* 2008;9:1225-1235.
3. Niculescu F, Rus HG, Retegan M, Vlaicu R. Persistent complement activation on tumor cells in breast cancer. *Am J Pathol* 1992;140:1039-1043.
4. Müller-Eberhard HJ. Molecular organization and function of the complement system. *Annu Rev Biochem* 1988;57:321-347.
5. Morgan J, Spendlove I, Durrant L. The role of CD55 in protecting the tumour environment from complement attack. *Tissue Antigens* 2002;60:213-223.
6. Gancz, D, Fishelson Z. Cancer resistance to complement-dependent cytotoxicity (CDC): problem-oriented research and development. *Mol Immunol* 2009;46:2794-2800.
7. Liu J, Miwa T, Hilliard B, Chen Y, Lambris J, Wells A, et al. The complement

- inhibitory protein DAF (CD55) suppresses T cell immunity in vivo. *J Exp Med* 2005;201:567-577,
8. Mikesch JH, Buerger H, Simon R, Brandt B. Decay accelerating factor (CD55): a versatile acting molecule in human malignancies. *Biochim Biophys Acta* 2006;1766:42-52.
 9. Guo RF, Ward PA. Role of C5a in inflammatory responses. *Annu Rev Immunol* 2005;23:821-852.
 10. Markiewski MM, Lambris JD. The role of complement in inflammatory diseases from behind the scenes into the spotlight. *Am J Pathol* 2007;171:715-727.
 11. DiScipio RG, Smith CA, Müller-Eberhard HJ, Hugli TE. The activation of human complement component C5 by a fluid phase C5 convertase. *J Biol Chem* 1983;258:10629-10636.
 12. Huber-Lang M, Sarma JV, Zetoune FS, Rittirsch D, Neff TA, McGuire SR, et al. Generation of C5a in the absence of C3: a new complement activation pathway. *Nature Med* 2006;6:682-687.
 13. Kasthuri RS, Taubman MB, Mackman N. Role of tissue factor in cancer. *J Clin*

Oncol 2009;27:4834-4838.

14. Huber-Lang M, Youkin EM, Sarma JV, Riedermann N, McGuire SR, Lu KT, et al. Generation of C5a by phagocytic cells. *Am J Pathol* 2002;161:1849-1859.
15. Gerard NP, Gerard C. The chemotactic receptor for human C5a anaphylatoxin. *Nature* 1991;349:614-17.
16. Zwirner J, Fayyazi A, Götze O. Expression of the anaphylatoxin C5a receptor in non-myeloid cells. *Mol Immunol* 1999;36:877-884.
17. Buchner RR, Hugli TE, Ember JA, Morgan EL. Expression of functional receptors for human C5a anaphylatoxin (CD88) on the human hepatocellular carcinoma cell line HepG2. Stimulation of acute-phase protein-specific mRNA and protein synthesis by human C5a anaphylatoxin. *J Immunol* 1995;155:308-315.
18. Coussens, LM, Werb Z. Inflammation and cancer. *Nature* 2002;420:860-867.
19. Balkwill, F. Cancer and the chemokine network. *Nat Rev Cancer* 2004;4:540-50.
20. Retz MM, Sidhu SS, Blaveri E, Kerr SC, Dolganov GM, Lehmann J, et al. CXCR4 expression reflects tumor progression and regulates motility of bladder

- cancer cells. *Int J Cancer* 2005;114:182-189.
21. Lian Z, Yoon Y, Votaw J, Goodman MM, William L, Shim H. Silencing of CXCR4 blocks breast cancer metastasis. *Cancer Res* 2005;65:967-971.
 22. Saur D, Seidler B, Schneider G, Algül H, Beck R, Senekowitsch-Schmidtke R, et al. CXCR4 expression increases liver and lung metastasis in a mouse model of pancreatic cancer. *Gastroenterology* 2005;129:1237-1250.
 23. Markiewski MM, Lambris JD. Unwelcome complement. *Cancer Res* 2009;69:6367-6370.
 24. Schraufstatter IU, Trieu K, Sikora L, Sriramarao P, DiScipio R. Complement C3a and C5a induce different signal transduction cascades in endothelial cells. *J Immunol* 2002;169:2102-2110.
 25. Albin A, Iwamoto Y, Kleinman HK, Martin GR, Aaronso SA, Kozlowski JM, et al. A rapid in vitro assay for quantitating the invasive potential of tumor cells. *Cancer Res* 1987;47:3239-3245.
 26. Hanazaki K, Kajikawa S, Shimosawa N, Shimada K, Hiraguri M, Koide N, et al. Prognostic factors of intrahepatic cholangiocarcinoma after hepatic resection:

- univariae and multivariate analysis. *Hepatogastroenterology* 2002;49:311-316.
27. Banks PN, Barker MD, Burton DR. Recruitment of actin to the cytoskeletons of human monocyte-like cells activated by complement fragment C5a. Is protein kinase C involved? *Biochem J* 1988;252:765-769.
28. Monk PM, Banks P. Evidence for the involvement of multiple signaling pathways in C5a-induced actin polymerization and nucleation in human monocyte-like cells. *J Mol Endocrinol* 1991;6:241-247.
29. Stetler-Stevenson WG, Aznavoorian S, Liotta LA. Tumor cell interactions with the extracellular matrix during invasion and metastasis. *Annu Rev Cell Dev Biol* 1993;9:541-573.
30. Singh S, Singh UP, Grizzle WE, Lillard JW Jr. CXCL12-CXCR4 interactions modulate prostate cancer cell migration, metalloproteinase expression and invasion. *Lab Invest* 2004;84:1666-1676.
31. Takafuji S, Ishida A, Miyakuni Y, Nakagawa T. Matrix metalloproteinase-9 release from human leukocytes. *J Invest Allergol Clin Immunol* 2003;13:50-55.

32. Nabha SM, dos Santos EB, Yamamoto HA, Belizi A, Dong Z, Meng H, et al. Bone marrow stromal cells enhance prostate cancer cell invasion through type I collagen in an MMP-12-dependent manner. *Int J Cancer* 2008;122:2482-2490.
33. Miyata Y, Iwata T, Maruta S, Kanda S, Nishikido M, Kaga S, et al. Expression of matrix metalloproteinase-10 in renal cell carcinoma and its prognostic role. *Eur Urol* 2007;52:791-797.
34. Kessenbrock K, Plaks V, Werb Z. Matrix metalloproteinases: regulators of the tumor microenvironment. *Cell* 2010;141:52-67.
35. Romualdez AG Jr, Ward PA. A unique complement derived chemotactic factor for tumor cells. *Proc Nat Acad Sci USA* 1975;72:4128-4132.
36. Orr W, Phan SH, Varani J, Ward PA, Kreutzer DL, Webster RO, et al. Chemotactic factor for tumor cells derived from the C5a fragment of complement component C5. *Proc Natl Acad Sci USA* 1979;76:1986-1989.
37. Schiefeldecker HL, Schlaf G, Koleva M, Götze O, Jungermann K. Induction of functional anaphylatoxin C5a receptors on hepatocytes by in vivo treatment of rats with IL-6. *J Immunol* 2000;164:5453-5458.

38. Takeyama H, Wakamiya N, O'Hara C, Arthur K, Niloff J, Kufe D, et al. Tumor necrosis factor expression by human ovarian carcinoma in vivo. *Cancer Res* 1991;51:4476-4480.
39. Maeda H, Fang J, Inutsuka T, Kitamoto Y. Vascular permeability enhancement in solid tumors: various factors, mechanisms involved and its implications. *Int Immunopharmacol* 2003;3:319-328.
40. Hall A. Rho GTPases and the actin cytoskeleton. *Science* 1998;279:509-514.
41. Nobes CD, Hall A. Rho, Rac, and Cdc42 GTPases regulate the assembly of multimolecular focal complexes associated with actin stress fibers, lamellipodia, and filopodia. *Cell* 1995;81:53-62.
42. Li Z, Hannigan M, Mo Z, Liu B, Lu W, Wu Y, et al. Directional sensing requires G $\beta\gamma$ -mediated PAK1 and PIX α -dependent activation of Cdc42. *Cell* 2003;114:215-227.

Figure legends

Figure 1. Expression of C5aR in human primary cancers. **A**, Human cancer tissues were immunohistochemically stained with an anti-C5aR antibody or control IgG (inset), and representative examples are shown. Colon cancer (top left) and normal colon epithelium (top right); esophagus normal epithelium (bottom, encircled) and cancer (bottom, not encircled). Scale bars = 50 μ m. **B**, Cancer cell C5aR-positive case ratios (positive cases/total cases examined) (\bullet) in primary organs. The vertical scale bar shows the 95% confidence interval that is estimated from the binominal proportion based on the beta distribution. EP, esophagus ($n = 20$); ST, stomach ($n = 20$); Col, colon ($n = 40$); Liv, liver ($n = 20$); BD, bile ducts ($n = 46$); Pan, pancreas ($n = 10$); Kid, kidney ($n = 11$); UB, urinary bladder ($n = 45$); Lun, lung ($n = 12$); PT, prostate ($n = 25$); Mam, mammary gland ($n = 21$).

Figure 2. Expression of C5aR on cancer cell lines including HuCCT1/C5aR and HuCCT1/mock. **A**, Expression of C5aR mRNA in several cancer cell lines shown by RT-PCR. **B**, Expression of C5aR protein in bile duct and colon cancer cell lines, shown

by immunoblotting using an anti-C5aR antibody. β -actin mRNA and protein were used as controls. **C**, Expression of C5aR on the cell membrane in MEC and HuCCT1/C5aR, shown by flow cytometry using FITC-conjugated anti-C5aR antibody (gray line) or control antibody (black line).

Figure 3. C5a elicits C5aR expressing cancer cells by inducing cytoskeletal reorganization and changes in cellular morphology. **A**, HuCCT1/C5aR and HuCCT1/mock cells were incubated with C5a (100 nM) and fixed at indicated time points. F-actin was visualized by immunofluorescence staining with Alexa 488-conjugated Phalloidin. Scale bars: 20 μ m. Arrow head and an arrow indicate filopodia and membrane ruffling, respectively. **B**, Time Lapse analysis of cell motility. Cell images taken at 0, 3, 6 and 9 h are shown. Broken circles indicate the initial cell position shown at 0 h. **C**, Cell migration distance was measured by tracing a cell. * $P < 0.01$ ($n = 6$).

Figure 4. Enhancement of C5aR-expressing cancer cell invasion by C5a *in vitro*.

Cancer cell invasion was measured by the Matrigel invasion chamber assay. HuCCT1-derived (**A**) or MEC cells (**B**) were placed in the upper chamber and medium supplemented with various concentrations of C5a was placed in the lower chamber. HuCCT1-derived (**C**) or MEC cells (**D**) were pretreated with various concentrations of C5a for 12 h and 24 h respectively. These cells were washed and were placed in the upper chamber, and medium was placed in the lower chamber. Incubation time for assay: 24 h (**A, C**) and 36 h (**B, D**). (□), HuCCT1/mock (**A, C**); (■), HuCCT1/C5aR (**A, C**); crosshatched and closed bars (**B, D**) indicate MEC cells treated with anti-C5aR antibody or nonspecific IgG, respectively. Gray bars (**A, B**) indicates cells incubated in the upper chamber in the presence of GM6001 (5 μ M). **E**. Checkerboard analysis for C5a cancer cell invasion activity. Closed, crosshatched and open bars indicate C5a concentration 0, 10 or 100 nM, respectively, in the lower chamber. *, $p < 0.01$; n.s., not significant.

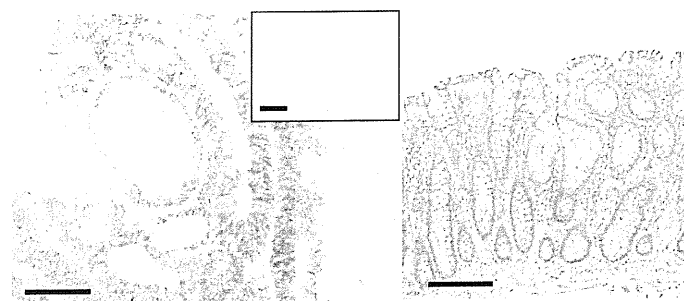
Figure 5. Enhanced invasiveness of C5aR-expressing cancer cells by C5a *in vivo*.

HuCCT1/C5aR and HuCCT1/mock cells were incubated separately in the presence or

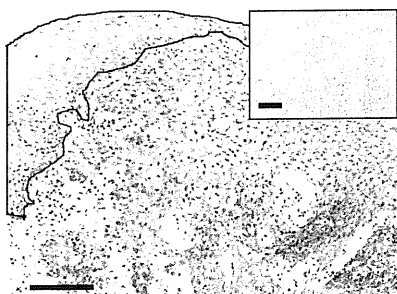
absence of 100 nM C5a (C5a(+)) or C5a(-), respectively) for 12 h. After washing, cells were labeled, mixed, and injected together into nude mouse skin. **A.** Distribution of HuCCT1/C5aR (*orange*) and HuCCT1/mock (*green*) cells in nude mouse skin two days after implantation. Right panels are corresponding sections stained with hematoxylin-eosin. Bars = 300 μ m. **B.** Cell distribution square ratio (HuCCT1/C5aR cells versus HuCCT1/mock cells). Cells were incubated in the presence (■) or absence (□) of C5a. *, $p < 0.01$ ($n = 5$).

Figure 1

A



colon



esophagus

B

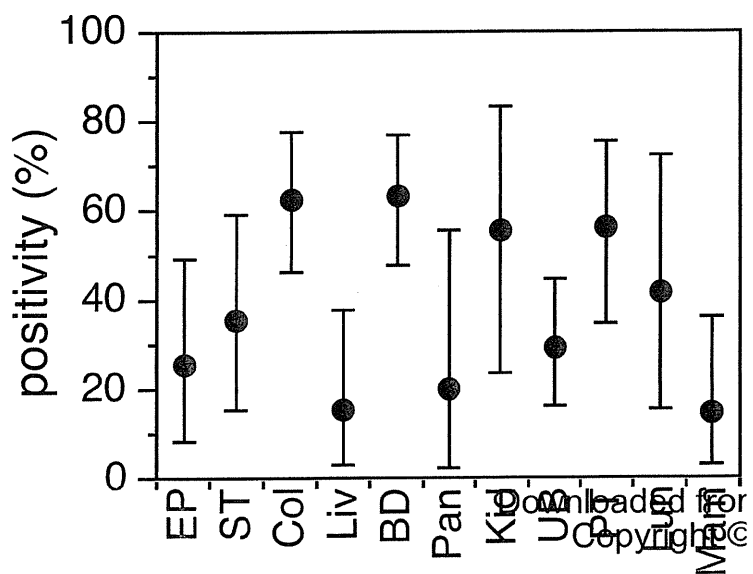
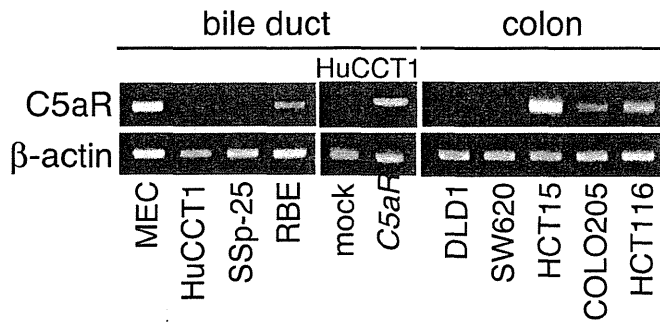
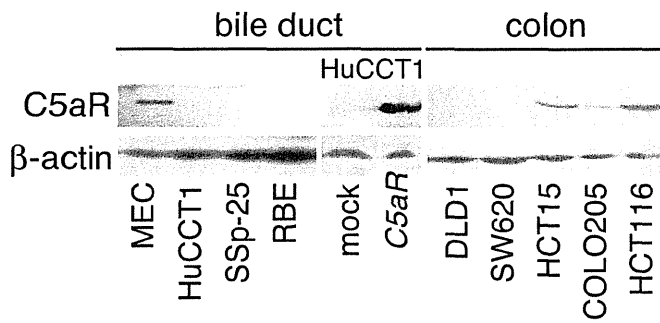


Figure 2

A



B



C

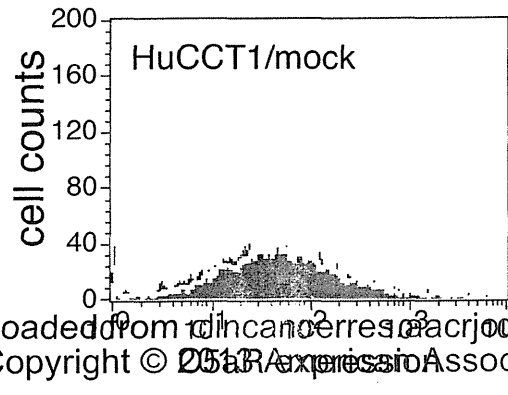
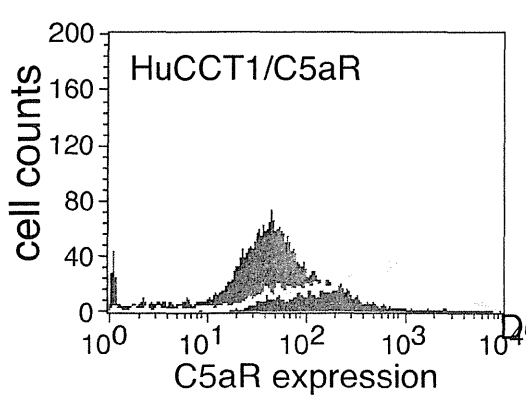
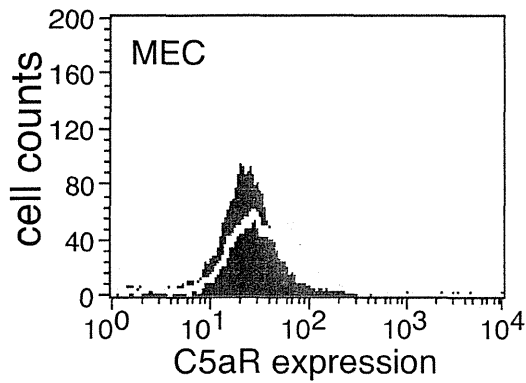
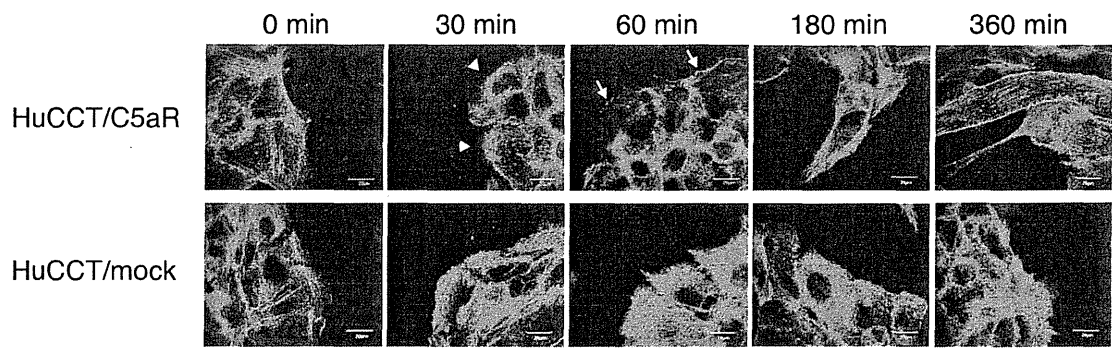
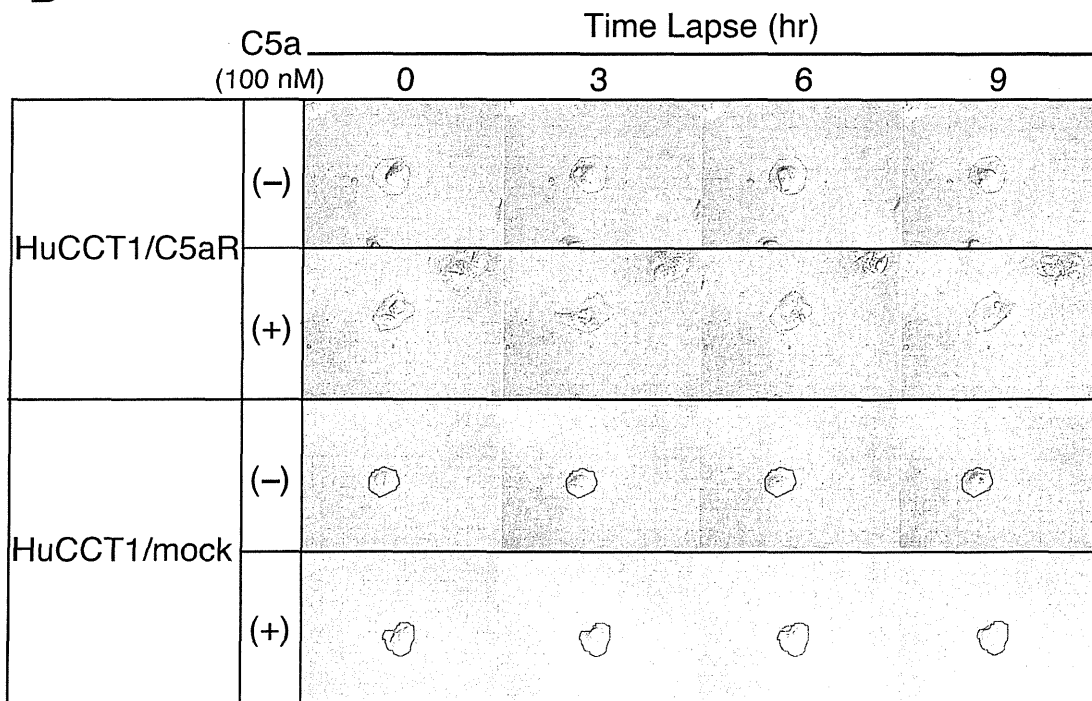


Figure 3

A



B



C

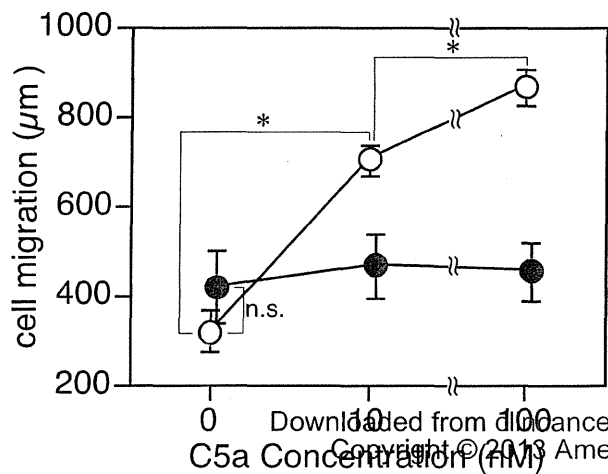
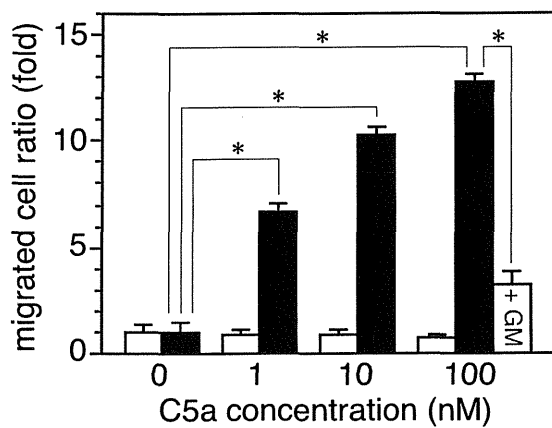
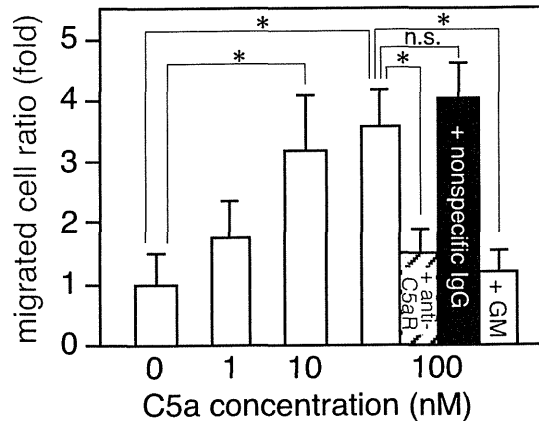


Figure 4

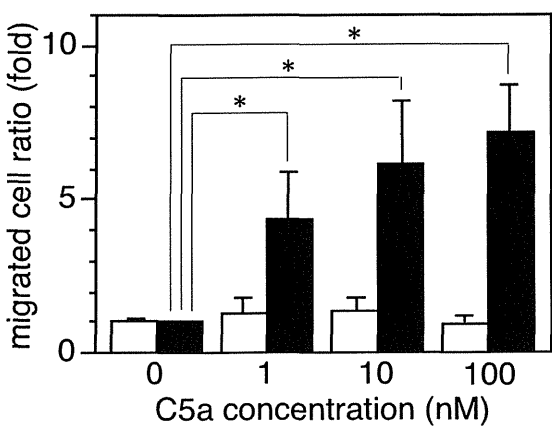
A



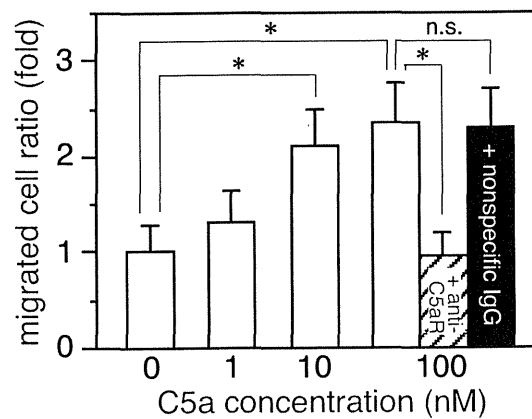
B



C



D



E

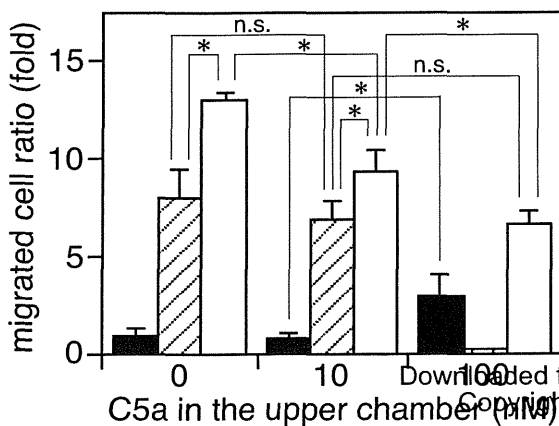
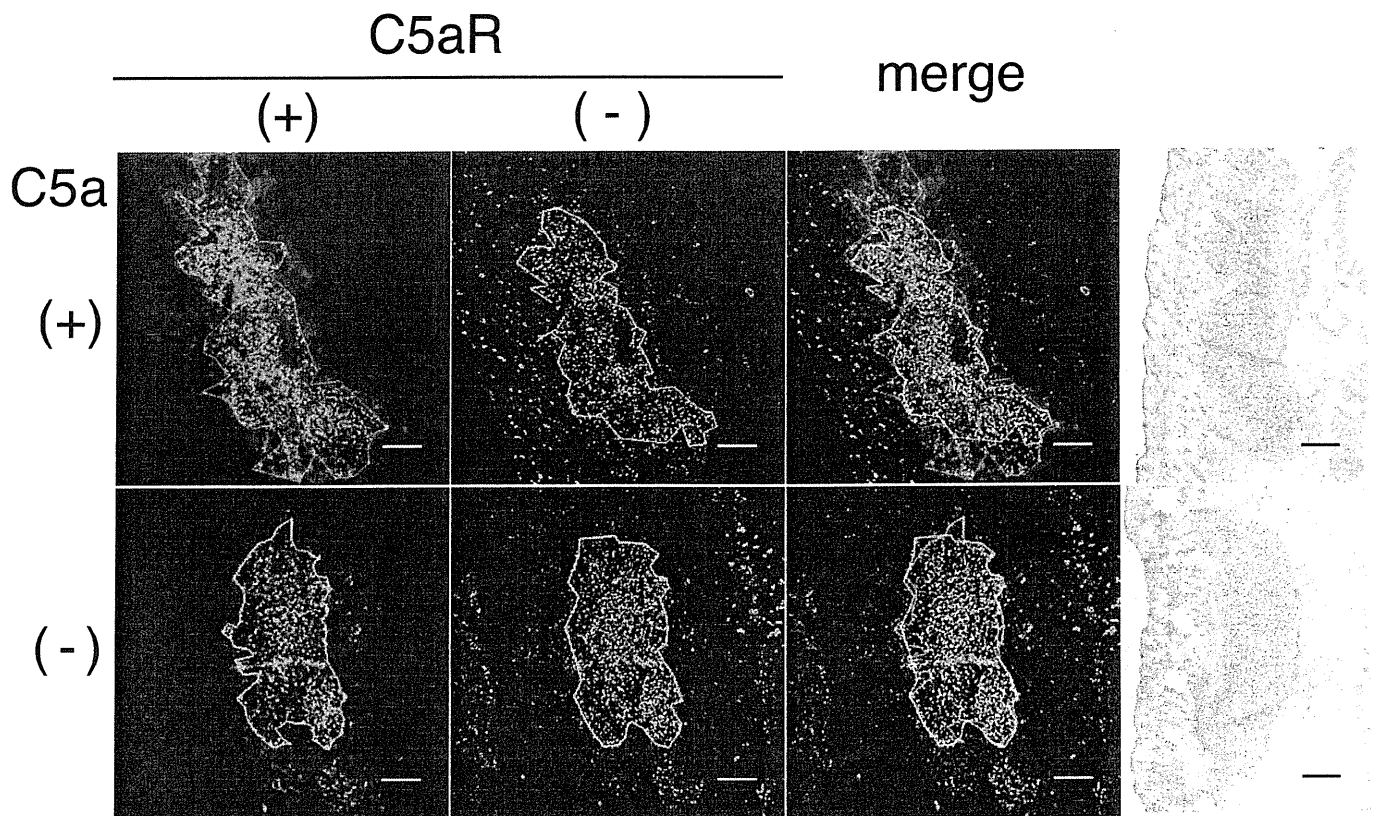


Figure 5

A



B

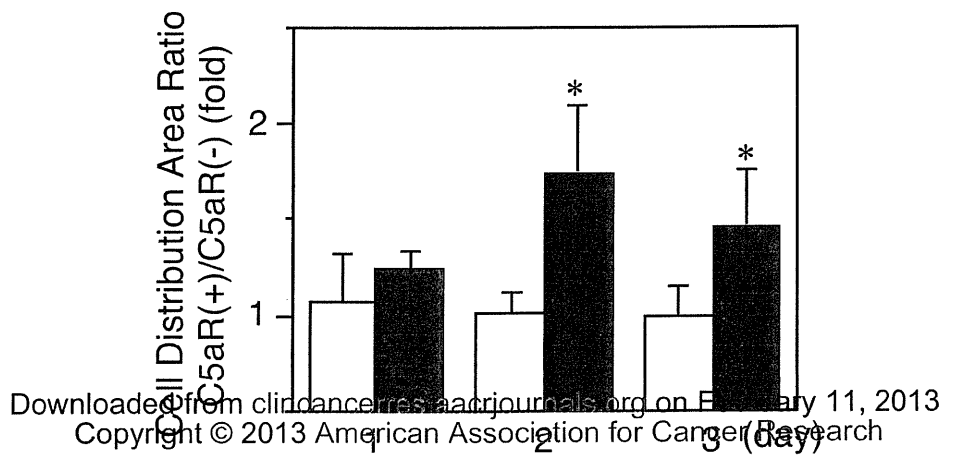


Table 1. C5a-stimulated MMP release from C5aR expressing cancer cells.

MMP	MEC			HuCCT1/C5aR		
	C5a (-) ^a	C5a (+) ^a	Ratio ^b	C5a (-) ^a	C5a (+) ^a	Ratio ^b
1	149332.6±17039	291140.4±5360.4*	1.95	88906.6±27436.8	129408±3485	1.46
2	32.5±11.3	116.9±67.8	3.59	1220.4±184.3	870.7±73	0.71
3	26.8±12.0	134.7±42.1*	5.03	971.6±224.6	927.5±162.9	0.95
8	20.1±23.6	74.9±29.9	3.72	335.6±77.7	1128.3±120.9*	3.36
9	< 0.1 ^c	12.3±3.6*	-	6105.1±2011.3	6213.4±4357.7	1.02
10	857.6±740.5	9301.4±641.8*	10.84	57641.4±5197.5	111666.4±7911.1*	1.94
13	359.2±118.7	1367.3±309.3*	3.80	1411.9±154.6	1642.8±287	1.16

^a MMP concentrations (pg/mL) in culture supernatants of cancer cells cultured for 24 h in the presence (+) or absence (-) of C5a (100 nM). ^b ratio of C5a(+) versus C5a(-) in mean values. ^c below the detection limit. **P* < 0.01 (*n* = 4).

A Case of Peritoneal Dissemination of High-grade Small Round Cell Sarcoma

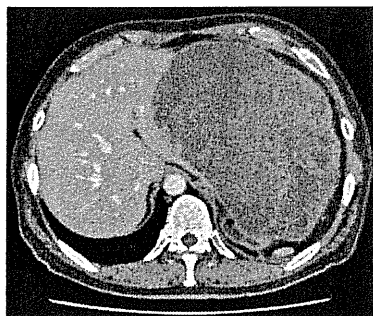


Figure 1.



Figure 2.

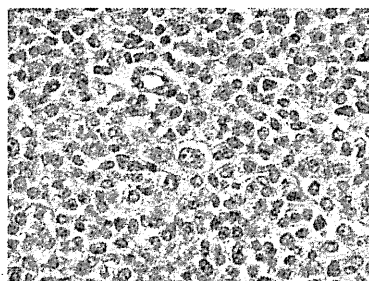


Figure 3.

A 46-year-old man, who had undergone resection of intra-abdominal tumor combined with part of the small bowel and ascending colon at another hospital 1 month before, was referred to our institution. After pathological examination of the resected specimen, the tumor was suspected to be high-grade small round cell sarcoma, presumably arising from the ileocecal mesentery. After referral to our hospital, six cycles of chemotherapy, composed of doxorubicin and ifosfamide, were administered, because imaging studies showed multiple residual intra-abdominal disseminations of the tumor. After chemotherapy, the size and number of the disseminative tumors had decreased. However, 6 months later, the patient complained of exaggerating left upper abdominal pain. Computed tomography (CT) and magnetic resonance imaging (MRI) demonstrated a rapidly enlarging mass of ~20 cm in diameter in the left subphrenic space (Fig. 1: axial CT image; Fig. 2: coronal MRI image). Intra-tumoral hemorrhage was suspected because laboratory tests showed progressive severe anemia (hemoglobin level declined to 5.9 g/dl). Although several other intra-abdominal tumors were recognized, excision of the largest subphrenic tumor was conducted in order to prevent tumor rupture and life-threatening bleeding. Total gastrectomy, left lateral bisegmentectomy (segments 2 and 3) of the liver and partial resection of the diaphragm were necessary for complete resection of the tumor.

Pathologically, the tumor consisted of small round cells with negative immunohistochemical reactivity for AE1/3, EMA and desmin. Finally, the diagnosis of high-grade small round cell sarcoma was made (Fig. 3).

The postoperative course was uneventful, but the patient died ~1 month after the surgery due to multiple liver metastases and rapid growth of residual tumors.

*Tsugumasa Kamata and Satoshi Nara
Hepatobiliary and Pancreatic Surgery Division
National Cancer Center Hospital
Tokyo, Japan*

doi:10.1093/jjco/hys198

S3-7 GEST 試験 (膵癌の第 III 相試験) の追跡調査結果報告

横浜市立大学附属市民総合医療センター消化器病センター¹, 国立がん研究センター中央病院肝胆膵腫瘍科², 静岡県立静岡がんセンター消化器内科³, 大阪府立成人病センター消化器検診科⁴, 神奈川県立がんセンター消化器内科⁵, 愛知県がんセンター中央病院消化器内科⁶, 九州大学病院がんセンター⁷, 杏林大学腫瘍内科⁸, 福岡山王病院膵臓内科⁹, 東京女子医科大学消化器外科¹⁰, 千葉県がんセンター消化器内科¹¹, 東北大学大学院消化器外科¹², 昭和大学病院腫瘍内科¹³, 東京大学大学院医学系研究科公共健康医学専攻生物統計学¹⁴, 九州大学大学院臨床・腫瘍外科¹⁵

杉森 一哉¹, 奥坂 拓志², 福富 晃³, 上野 秀樹², 井岡 達也⁴, 大川 伸一⁵, 朴 成和³, 山雄 健次⁶, 水元 一博⁷, 古瀬 純司⁸, 船越 顕博⁹, 羽鳥 隆¹⁰, 山口 武人¹¹, 江川 新一¹², 佐藤 温¹³, 大橋 靖雄¹⁴, 田中 雅夫¹⁵

【目的】切除不能進行膵癌に対してゲムシタピン (GEM) 単独療法を対照として, TS-1 単独療法の生存期間における非劣性, ゲムシタピン + TS-1 (GS) 併用療法の生存期間における優越性を検証した. 本試験結果は 2011 年の ASCO および本学会にて報告を行ったが, 今回追跡調査を実施したので報告する.

【方法】GEM 群, TS-1 群は添付文書の用法・用量に従い投与が行われた. GS 群は 1,000mg/m² の GEM を 1, 8 日目に点滴静注し, TS-1 は体表面積に合わせた規定量 (60mg, 80mg, 100mg/日) を 14 日間連続投与し, その後 7 日間休薬する 21 日を 1 コースとしたスケジュールで実施した. 2011 年 7 月までのデータを使用して解析した.

【成績】本追跡調査解析時のイベント数は 832 例 (FAS) 中 795 イベントであった.

(1) MST は GEM 群 8.8 カ月 (95% CI : 8.0-9.7), TS-1 群 9.7 カ月 (95% CI : 7.6-10.8) であった (OS HR = 0.96, 97.5% CI : 0.79-1.17, p < 0.001 非劣性).

GS 群の MST は 9.9 カ月 (95% CI : 9.0-11.2) であった (OS HR = 0.91, 97.5% CI : 0.75-1.11, p = 0.28 優越性).

(2) サブグループ解析では, 局所進行例と PS1 症例で GS 群は良好な傾向を示した. 局所進行例の MST は GEM 群 12.7 カ月 (95% CI : 9.7-14.9), GS 群 15.9 カ月 (95% CI : 13.0-19.7, HR = 0.72, 95% CI : 0.51-1.03), PS1 の MST は GEM 群 6.2 カ月 (95% CI : 4.9-8.3), GS 群 9.6 カ月 (95% CI : 8.0-10.9, HR = 0.62, 95% CI : 0.46-0.83) であった.

【結論】TS-1 の GEM に対する非劣性の証明が再確認された. GS 療法は更なる検討の余地がある.

S3-8 進行膵癌に対するレニンアンギオテンシン系 (RA) 抑制による治療成績向上の試み

東京大学医学部消化器内科¹, 日本赤十字社医療センター消化器内科², 東京警察病院消化器内科³, JR 東京総合病院消化器内科⁴, 関東中央病院消化器内科⁵
中井 陽介¹, 伊佐山浩通¹, 伊地知秀明¹, 佐々木 隆¹, 伊藤由紀子², 松原 三郎³, 八木岡 浩⁴, 永野 里枝⁵, 川久保和道¹, 木暮 宏史¹, 山本 夏代¹, 笹平 直樹¹, 平野 賢二¹, 多田 稔¹, 小池 和彦¹

【目的】血管新生など腫瘍増殖を促す RA 系は, 膵癌における新たな治療標的として期待されている. 我々は, Gemcitabine (GEM) 療法を施行した進行膵癌 155 例の後向き解析にて, RA 系の抑制による良好な治療成績の可能性を報告した (Br J Cancer. 2010; 103: 1644-8). 今回 GEM・Candesartan (Can) 併用療法の第 1 相試験・多施設共同第 2 相試験を報告する. 【方法】[phase1] 正常血圧の進行膵癌に対する GEM・Can 併用療法の第 1 相試験として, GEM1000mg/m² 3 投 1 休に加えて Can 4, 8, 16, 32 mg の 4 Level を day1-28 に 1 日 1 回内服のスケジュールとした. Grade4 骨髄抑制, grade2 血圧低下・腎機能障害, その他の grade3 非骨髄抑制の有害事象を DLT とした. [phase2] phase1 で決定した推奨投与量 (RD) のスケジュールに基づき, 高血圧症例を含めた進行膵癌を対象に, 安全性・有効性を評価した. Can は, 正常血圧例で 16mg, 高血圧例で 8mg を開始, 血圧低下がない場合 16mg に増量した. 【結果】[phase1] 09 年 7 月~10 年 10 月に局所進行 7 例/遠隔転移 7 例の 14 例を登録 (Level 1 3 例, Level2 3 例, Level3 6 例, Level4 2 例), Level 3 にて grade4 好中球減少 (1/6 例), Level4 にて grade 2 血圧低下 (2/2 例) を認め, Can の推奨投与量は 16mg に決定. 奏効率 (RR) は 0% であったが, Disease control rate (DCR) は 79%, 無増悪生存期間 7.6 カ月, 全生存期間 22.9 カ月と良好な結果が得られた. [phase2] 11 年 5 月~11 年 12 月に進行膵癌 35 例 (局所進行 9 例/遠隔転移 26 例) を登録. grade3 以上の主な重篤な有害事象は, 骨髄抑制 (好中球減少 24%/血小板減少 18%) を認め, Can による有害事象として, grade2 血圧低下 2 例を 2 コースで認めたが, Can 減量により軽快. 観察期間 3.1 カ月と短いものの, RR は 13%, DCR63% と期待できる結果が得られた. 【結語】進行膵癌に対する GEM・Can 併用療法は安全かつ有効な可能性が示唆され, RA 系抑制は予後改善へ向けた有効な戦略となりうると考えられた.